PAPER

Circularly Polarized Rounded-Off Triangular Microstrip Line Array Antenna

David DELAUNE[†a)], ***Student Member***, **Josaphat Tetuko SRI SUMANTYO**[††], **Masaharu TAKAHASHI**[†††], ***and*** **Koichi ITO**[†††], ***Members***

SUMMARY The Japan Aerospace Exploration Agency (JAXA) plans to launch a geostationary satellite called Engineering Test Satellite VIII (ETS-VIII) in FY 2006. In this paper, a microstrip line array antenna, which has a very simple structure, is introduced to radiate a circularly polarized wave aiming at ETS-VIII applications. This antenna consists of a triangular conducting line with its vertexes rounded off, located above a ground plane, with a gap on one of its side to produce a circular polarization. The proposed antenna is analyzed by numerical simulations for a single element as well as for a three elements array configuration and the possibility of beam-switching in the azimuth space is experimentally confirmed in the latter case. It is found that by properly feeding the elements constituting the array antenna, for an elevation angle $El = 48°$ in Tokyo area, three beams are created in the conical-cut direction with a minimum gain more than 6.6 dBic and an axial ratio less than 3 dB.

key words: *microstrip line antenna, circular polarization, triangular shape, rounded vertex, array configuration, beam-switching, mobile satellite communications*

1. Introduction

The interest in the mobile satellite communications system technologies is expected to increase with the launch of the Japan Aerospace Exploration Agency's (JAXA) Engineering Test Satellite VIII (ETS-VIII). Among its applications, ETS-VIII will conduct orbital experiments on mobile satellite communications in the S-band [1]. One of the experimental aims is the development of a technology enabling the transmission and reception of multimedia information such as voice and images by use of the geostationary satellite for land mobile systems. Although the required specifications depend on the services and systems available, a small and light antenna having a high gain on a wide angular range is desired.

Up to this point, several antennas able to meet these requirements have been extensively investigated, are widely available in the literature [2], and include the conical beam antennas and the satellite-tracking antennas. The attractive feature of the former antenna design is that, as the radiation is omnidirectional in the conical-cut direction and the beam is broad in the elevation plane, satellite tracking is not necessary in the elevation plane. However, high gain cannot be achieved because of the isotropy in the conical-cut direction. In contrast, one of the advantages of the latter antenna is that the beam generated by satellite-tracking systems is always directed towards the satellite position even when the azimuth of the mobile station changes [3]. Therefore, such antennas have the possibility to reach a higher gain as compared to the conical beam antennas.

Hence, the authors have researched and presented simple on-board satellite-tracking circularly polarized array antennas for single [4], [5] and dual frequency [6]–[8], aimed at ETS-VIII applications. However, although the aforementioned antennas can satisfactorily be used in outdoor experiments [8], their size is relatively large. Consequently, in this paper, the authors propose a more compact satellite-tracking microstrip line array for ETS-VIII based on the notion of wire antenna [9].

Here, a microstrip line array antenna which has a very simple structure is introduced to radiate a circularly polarized wave. This antenna consists of a triangular conducting microstrip line, whose tips are rounded off, placed above a ground plane and with a gap on one of its side to produce a circular polarization [10]–[14]. The tips are rounded off so that a uniform current distribution is ensured and an impedance mismatch around the vertexes avoided. The proposed element and its array configuration are analyzed by numerical simulations and the possibility of beam-switching in the azimuth space is experimentally confirmed.

2. Specifications and Objectives

Table 1 shows the specifications and objectives of an antenna for mobile satellite communications aimed at ETS-VIII applications [4]–[8]. In this research, a thin miniaturized antenna for ETS-VIII and designed for a hundred kbps data transfer is analyzed. In this case, the necessary minimum gain on the azimuth space is set to more than 5 dBic with a maximum axial ratio over the investigated angular range set to less than 3 dB [6]–[8]. In addition, in this study, the measurements are assumed to take place in the center of Tokyo (elevation angle El of the geostationary satellite 48°). Furthermore, the operating frequency is fixed at 2.5025 GHz.

Manuscript received June 29, 2005.
Manuscript revised November 2, 2005.

[†] The author is with the Graduate School of Science and Technology, Chiba University, Chiba-shi, 263-8522 Japan.
[††] The author is with the Center for Environmental Remote Sensing, Chiba University, Chiba-shi, 263-8522 Japan.
[†††] The authors are with the Research Center for Frontier Medical Engineering, Chiba University, Chiba-shi, 263-8522 Japan.
a) E-mail: delaune.david@graduate.chiba-u.jp

DOI: 10.1093/ietcom/e89–b.4.1372

Table 1 Specifications and objectives of the antenna for ETS-VIII.

SPECIFICATIONS		
Frequency bands	Transmission (Tx)	2655.5 MHz to 2658.0 MHz
	Reception (Rx)	2500.5 MHz to 2503.0 MHz
Polarization	Left-handed circular polarization for both Tx and Rx	
OBJECTIVES		
Angular ranges	Elevation angle (*El*)	48° (Tokyo)
	Azimuth angle (*Az*)	0° to 360°
Minimum gain	more than 5 dBic	
Maximum axial ratio	less than 3 dB	

3. Structure of the Antenna

Figure 1 shows the configuration of the triangular microstrip line array antenna, whose tips are rounded off, placed above a ground plane. It is necessary to round off the tips of the triangular microstrip line, else the current launched from the feeding probe will be reflected by the vertexes as their inner angle is sharp and this would generate a standing wave that perturbs the current flow. Consequently, by rounding off the tips of the triangular line, a uniform current distribution is ensured and an impedance mismatch around the vertexes avoided. Although various shapes can be considered [10]–[23], the triangular one is chosen so that it can easily be made and the current distribution on the line can be controlled by changing the gap width and the perimeter. The center of the feeding probe (SMA connector with a long inner part) that connects the ground to the antenna element is located at 1 mm from the gap.

In order to induce circular polarization and sufficient gain, the antenna comprises three single-fed elements with a gap in one of their sides. The elements of the antenna are sequentially rotated [24] by 120° so that the gap is located outwards compared to the center of the array ensuring no adverse influence on the adjacent elements that would decrease the performances. Moreover, by sequentially rotating the elements, the relative phase between them is physically shifted. Therefore, assuming the phase of the first one is 0°, when rotating the others of 120° relatively to the center of the array antenna, phases of elements 2 and 3 are 120° and 240°, respectively. Such a sequential rotation ensures the generation of circular polarization. Furthermore, by use of the sequential rotation technique, there is a possibility of miniaturization of the antenna.

Figures 1(a) and (b) show the top view and side view of the designed array, respectively. Here, the antenna is made of a thin conducting microstrip line of width w etched on a high relative permittivity substrate whose thickness is t_1. Additionally, one element has a side l. Hence a perimeter L given by

$$L = 3l - \Delta s \quad (1)$$

where Δs is the gap width. The distance between the center

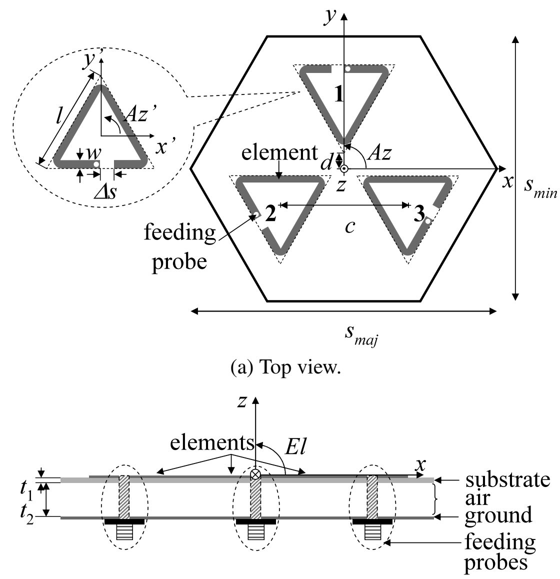

(a) Top view.

(b) Side view.

Fig. 1 Composition of the antenna.

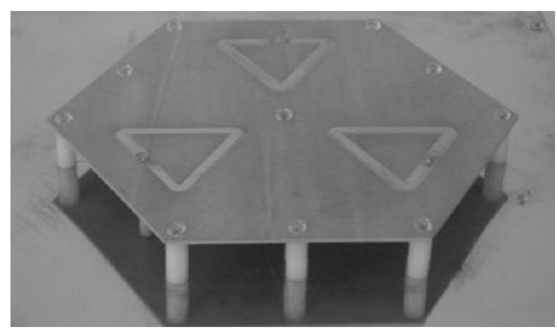

Fig. 2 External view of the fabricated antenna.

of the array and the tip of a triangle is d. The distance c between two centroids is then

$$c = \sqrt{3}(d + l/\sqrt{3}) \quad (2)$$

The ground plane and the substrate are separated by an air layer whose height is t_2. The height uniformity is ensured by means of plastic spacers. Finally, the substrate size has a hexagonal shape with its major and minor diagonals being s_{maj} and s_{min}, respectively.

The antenna is placed for the measurements on a ground plane whose size is 200 mm × 200 mm. An external view of the fabricated antenna is displayed in Fig. 2 and the beam-switching arrangement is shown in Fig. 3. Figure 3(a) shows the theoretical concept and Fig. 3(b) shows the process followed during the measurement. Switching is realized by successively turning off the feed sources of elements 1 to 3. The direction of the created beam is shifted in the azimuth plane by −90° from the element that is turned off for a left-handed circularly polarized antenna [4]–[8]. In Fig. 3, as an example, if element 2 is turned off (experimentally terminated in 50 Ω as explained in the next section), a wide beam is created in the direction $Az = 120°$. The

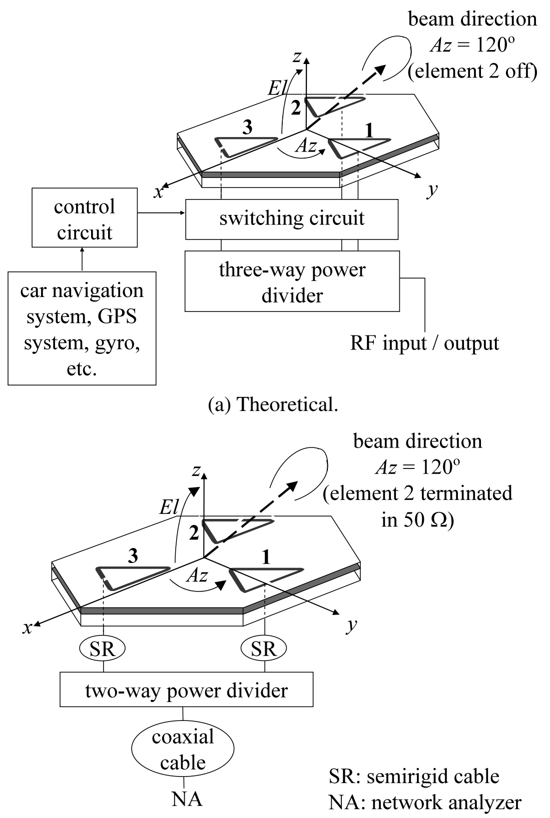

(a) Theoretical.

(b) Experimental.

Fig. 3 Outline of the system.

same method is applied to the other elements (1 and 3 alternatively off). As a result, switching all three beams in the conical-cut direction for each element can cover the whole azimuth range.

Information concerning the satellite position can be obtained by use of systems such as car navigation, GPS, gyro, etc. Although not discussed in this paper, the electronic circuit that controls the antenna and selects the elements to be turned on or off, makes use of the previously obtained information. In order to control the elements, switching circuits based on PIN diodes [25], [26] or switching ICs can be used.

4. Performance of the Antenna

The Method of Moments (MoM) has been chosen in the analysis for its asset of fast calculation. Owing to the software characteristics, the dielectric substrate and the ground plane are considered to be infinite. As the microstrip line antenna is backed by a perfectly conducting ground plane of an infinite extent that acts as a reflector, this antenna can be handled by the method of image.

In the next subsections, the condition for circular polarization is explained at first. Then a single element and the case of the three elements array antennas are analyzed and experimental results are shown in the case of the array. Precisely, the frequency characteristics of the impedance and antenna performances are shown. Finally, the results in terms of gain and axial ratio in both the elevation plane and the conical-cut direction are presented. The performances are compared with measurements realized in the radio anechoic chamber of the Graduate School of Science and Technology, Chiba University, Japan.

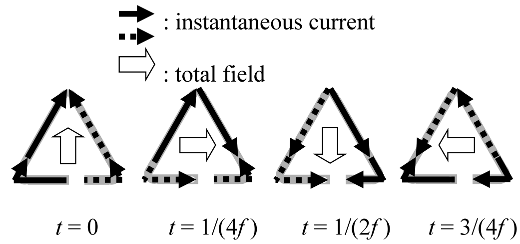

Fig. 4 Instantaneous current distribution and polarity.

It should be noted that during measurements, the actual switching network was not included because this paper focuses on the fundamental behavior and characteristics of the antenna. Instead, the switching process was performed by manually changing the elements to be fed or not, as explained in Sect. 3. Practically, when element 2 was investigated, elements 1 and 3 were connected to a two-way power divider by means of semi-rigid cables and element 2 was terminated in 50 Ω (see Fig. 3(b)).

4.1 Condition for Circular Polarization

Before dealing with the array configuration, it is necessary to have a traveling wave current distribution which has a constant amplitude and a linearly changing phase for a single loop antenna to radiate a circularly polarized wave. In the case of a circular loop, a circularly polarized wave can be radiated by means of loading a reactance of an appropriate value [15]. Instead of loading an appropriate reactance, a very simple method is to use a gap [10]–[14]. It has been shown theoretically that by introducing such a gap with a certain width on the printed element and feeding the antenna with a coaxial probe, a traveling-wave current distribution could be excited, and as a result, a circular polarization can be achieved.

Fundamentally, using the line electric-current source method, the way of the proposed antenna to radiate circular polarization can be easily understood. Assuming one element to be fed from the bottom left part compared to the gap location as in Fig. 1. The instantaneous current distribution is shown by the arrows in Fig. 4 where the arrows point in the opposite direction every half guide wavelength λ_g. From this figure, at time $t = 0$, the total radiation field from each segment consists of the juxtaposition of the current flowing on the left and right segments of the triangular line, because the radiated fields of the horizontal segment at the bottom cancel each other out. Hence the radiated field is upwards directed in the plane where the element lays. When $t = 1/(4f)$, where f is the frequency, the total radiation field will be of horizontal right-oriented polarity. Similarly, when $t = 1/(2f)$ or $t = 3/(4f)$, the polarity of the total radiation field will be oriented downwards or to the left, respectively. As shown in the figure, the polarity of the total field of the radiated electromagnetic waves (normal to the surface of the paper), rotates clockwise, and completes one cycle in time $1/f$. Thus, the fundamental element of the antenna operates as a left-handed circularly polarized antenna.

4.2 Application to a Single Element

4.2.1 Composition

The theory described above is confirmed after by numerically analyzing a single element thus proving the generation of a circularly polarized wave. The parameters, deduced from various analyses not explicitly shown here for reason of shortening, are summarized in Table 2. In order to show the influence and necessity of rounding off the tip of the triangular microstrip line, two cases are numerically analyzed: triangular microstrip with and without rounded vertexes.

4.2.2 Input Characteristics

Figure 5 shows the S-parameters. From this figure, the S-parameters tend to improve when the vertexes are rounded off. It is due to the fact the impedance mismatch is avoided or at least decreased around the rounded tips, as previously stated. Indeed by rounding the tip, the line width w is always constant even around the vertex, when the value of the line width would be $2w$ in case the vertex is straight.

Table 2 Antenna parameters (single element).

	Symbol	Value (straight vertexes)	Value (rounded vertexes)
Relative permittivity	ϵ_r	9.80	9.80
Loss tangent	$\tan\delta$	0.003	0.003
Substrate thickness	t_1	1.27 mm	1.27 mm
Air thickness	t_2	14.00 mm	14.00 mm
Element side	l	39.14 mm	40.54 mm
Line width	w	3.00 mm	3.00 mm
Gap width	Δs	1.00 mm	1.00 mm

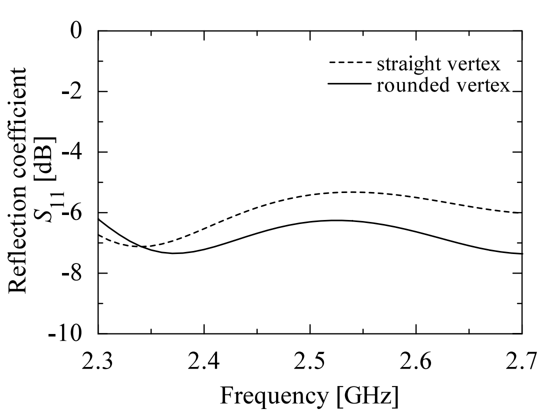

Fig. 5 S-parameters (single element).

4.2.3 Radiation Characteristics in the Elevation Plane

Figure 6 represents the radiation characteristics in the elevation plane for a single element in terms of gain and axial ratio. Figure 6(a) shows the results in the $Az' = 0°$ to $180°$ plane while Fig. 6(b) shows the performances in the $Az' = 90°$ to $270°$ plane. From both figures, it is obvious that the use of rounded vertexes improves the antenna performances. In Fig. 6(a), the minimum axial ratios are 1.6 dB and 0.7 dB for straight and rounded vertexes, respectively. An improvement of 5° in the 3 dB-axial ratio beamwidth can be observed as well. In Fig. 6(b), the minimum axial ratio drops from 1.1 dB to 0.5 dB with an increase of 10° in the 3 dB-axial ratio beamwidth when the vertexes are rounded off. From these results, it can be said that the use of rounded vertexes improves the current distribution.

As a conclusion, it has been shown that a single triangular microstrip line antenna element radiates a circularly polarized wave when its constituting tips are rounded off, ensuring a uniform current distribution and an impedance mismatch avoidance.

In the next step, the single element antenna is put into an array configuration and the obtained results are presented in the following section.

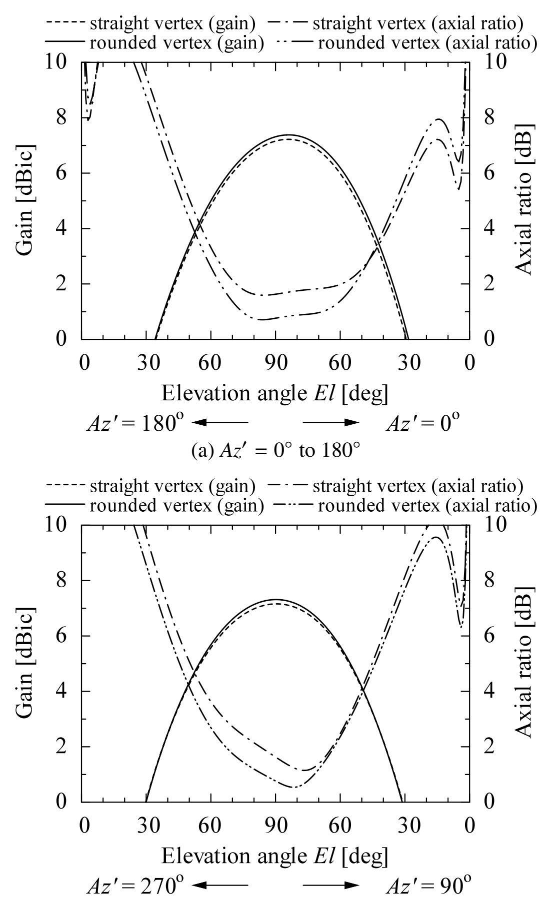

Fig. 6 Radiation characteristics in the elevation plane.

4.3 Case of the Array Antenna

4.3.1 Parameters Analysis

It has been shown above that a single element can radiate a circularly polarized wave provided that proper parameters are used. In this section, the case of the array is analyzed in details and it is clarified here that suitable parameters for the perimeter of the line, the gap width, the distance between adjacent elements, and the air thickness exist to radiate a circularly polarized wave.

The parameters of the line considered are deduced from the variations of the perimeter L, the gap width Δs and the distance between the center of the array and the tip of one element d. Figures 7 and 8 show the axial ratio characteristics as a function of L and Δs, respectively. In this research, the air thickness t_2 is fixed to 14 mm ($0.12\lambda_0$) as for the case of a single element in order to decrease the number of parameters to be analyzed. In these graphs, the axial ratio is examined in the case El = 48° and Az = 120° (i.e. element 2 off).

Figure 7 shows the axial ratio when L is changed for various values of d. In the present case, the value of Δs is fixed to 3.0 mm. From this figure, good axial ratios for circular polarization are obtained for appropriate values of L. In addition, it can be seen that the perimeter decreases with an increase in d. This is explained by the fact that the mutual coupling between elements decreases along with the increase in d.

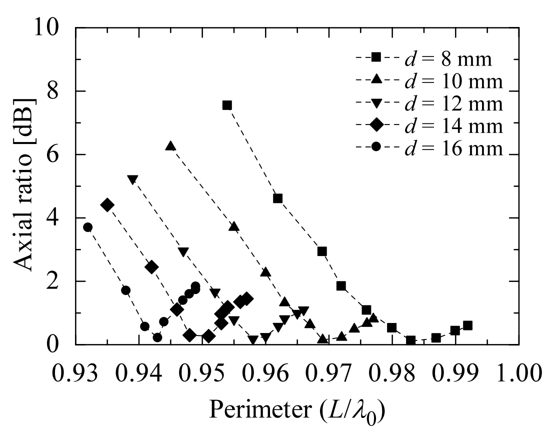

Fig. 7 Axial ratio characteristics vs. perimeter (Az = 120°, El = 48°).

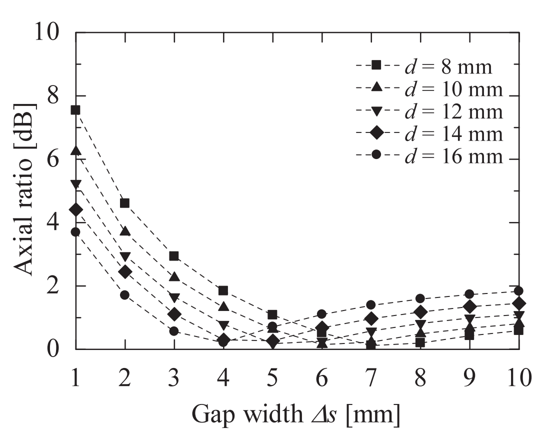

Fig. 8 Axial ratio characteristics vs. gap width (Az = 120°, El = 48°).

Figure 8 shows the variation of axial ratio when Δs is changed. Here, the value of L is optimized every time so that the axial ratio is minimal at the targeted operating frequency and the so obtained value of L is used for each Δs. From this figure, it can be seen that the axial ratio decreases until a minimum value then increases with an increase in Δs. It comes from the fact the antenna gets very inductive with an increase in Δs, which induces a decrease in the axial ratio as stated in [15]. Hence the value of Δs should be chosen neither too large nor too small.

From these graphs, aiming at an element and antenna global size as small as possible (i.e. the antenna should be contained within a diameter of 100 mm from the array center to the bottom edge of an element), as well as an input impedance where X_{in} is as close as possible to 0 and axial ratio performances as low as possible (typically less than 2 dB), the array antenna whose parameters are summarized in Table 3 is numerically and experimentally analyzed in the next sections. Use of the proposed configuration allows a decrease of about 20% in the surface of a single element compared to previously [6]–[8], with the distance c between two centroids being about $0.51\lambda_0$, where λ_0 is the wavelength in free space.

4.3.2 Input Characteristics

Figures 9 and 10 show the input characteristics of the antenna, i.e. S-parameters and input impedance, respectively. The input characteristics of the antenna are measured at the input of the probe that is soldered to the ground (i.e. the admittance of the probe is not included in the result) in case of element 2 only, or at the input of the power divider in the case of the array (element 2 terminated in 50 Ω). In Fig. 9, the measurement and the simulation present the same tendency. The measurement results are slightly better than the

Table 3 Antenna parameters (array configuration).

	Symbol	Value
Relative permittivity	ϵ_r	9.80
Loss tangent	$\tan\delta$	0.003
Substrate thickness	t_1	1.27 mm
Air thickness	t_2	14.00 mm
Element side	l	40.76 mm
Line width	w	3.00 mm
Gap width	Δs	3.00 mm
Distance between center of the array and tip of the element	d	12.00 mm
Substrate major diagonal	s_{maj}	140.00 mm
Substrate minor diagonal	s_{min}	120.00 mm

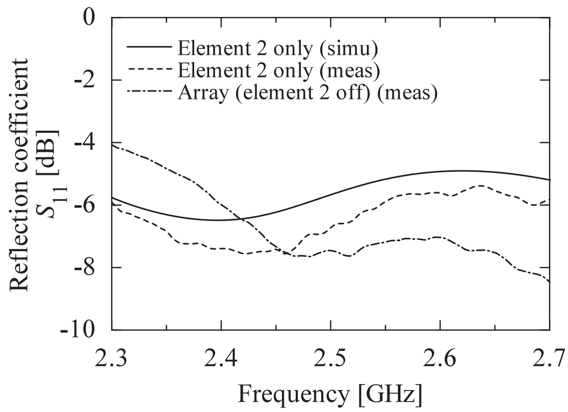

Fig. 9 S-parameters (array configuration).

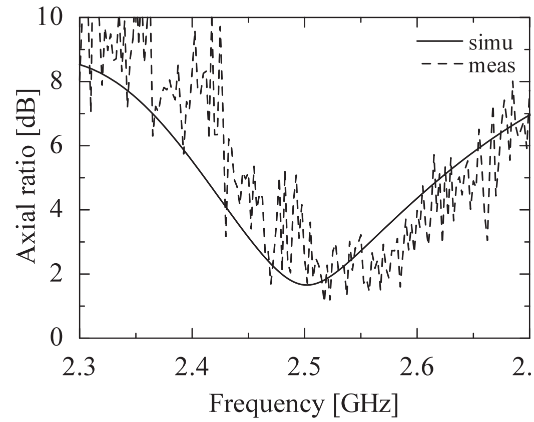

Fig. 11 Frequency performances (Az = 120°, El = 48°).

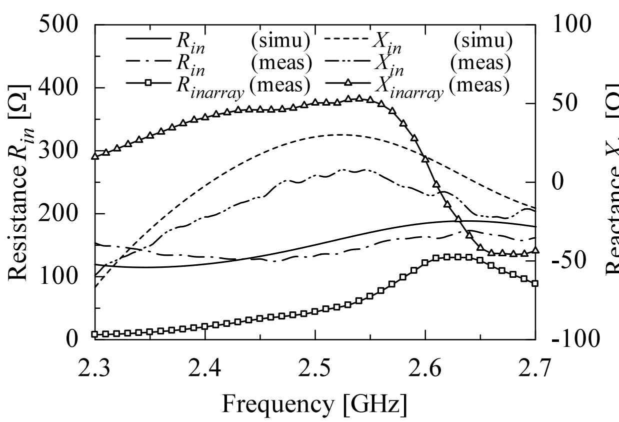

Fig. 10 Input impedance (array configuration).

simulation due to the accuracy in the fabrication of the antenna. Although not explicitly shown here, the input characteristics tend to be better with a decrease in t_2 to a certain extent. During the fabrication, it appears that t_2 was slightly lower than its simulated value hence explaining the improvement. In addition, from the same figure, when the power divider is used, improvement is realized due to the inner properties of the power divider, which is a Wilkinson divider.

In Fig. 10, the resistance and reactance are shown. The full line and dashed line represent the real part (resistance R_{in}(simu)) and the imaginary part (reactance X_{in}(simu)) by simulation while the dash single-dotted line and the dash double-dotted line show their counterpart R_{in}(meas) and X_{in}(meas) obtained by measurement. Additionally, in the case of the array (element 2 off), the square and triangle plotted lines represent the resistance $R_{inarray}$(meas) and reactance $X_{inarray}$(meas), respectively. Only the case of element 2 is presented for reason of graph legibility. The slight improvement in the results of measurement compared to the simulation can be explained by the same reason as above. From this figure, it appears the input impedance is about 150 Ω in the case of an element measured independently. During the measurement of the radiation patterns, as the inactivated element is terminated by 50 Ω, a mismatch can occur and the phenomenon of reradiation from the terminated element that acts as a parasitic might happen. However, for actual use, the antenna will eventually be backed by a switching circuit to control the element to be turned off. Hence even if the antenna impedance is not 50 Ω, a method to eliminate the problem of reradiation is to use 150 Ω lines for the switching circuit rather than 50 Ω lines.

4.3.3 Frequency Characteristics

The antenna was numerically optimized by minimizing the axial ratio at El = 48° based on simulations for the targeted receive frequency as shown in Fig. 11, in the case element 2 off. The axial ratio is 1.7 dB at 2.5025 GHz. In the same figure, it can be seen that measured results follow the same tendency with a shift of 15 MHz in the upper frequency and a narrowing in the bandwidth. This shifting is explained by the influence of the ground plane which is finite in the case of measurement while it is infinite by numerical simulations [4], [5]. Note that the rippling can be explained by the ground plane effect and by the fact the number of points used for the averaging might have been too small.

4.3.4 Radiation Characteristics in the Elevation Plane

Figure 12 shows the radiation characteristics of the antenna in the elevation plane when element 2 is off (in the direction Az = 120° to 300°). The full line and dashed line represent the results obtained by numerical simulation and measurement, respectively. Figure 12(a) shows that the maximum of radiation occurs when El = 63° for the numerical simulation and El = 64° for the measurement. Additionally, in Fig. 12(b) it can be observed that the axial ratio obtained by numerical analysis and by measurement is satisfactorily less than 3 dB at 48°. The beam narrowing, especially in the case of the axial ratio, is due to the influence of the finiteness of the ground plane.

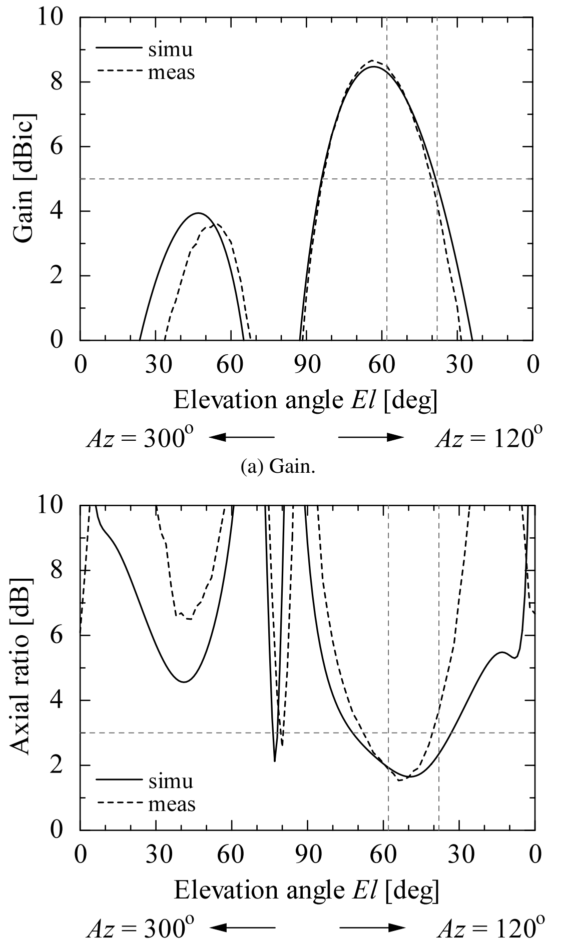

(a) Gain.

(b) Axial ratio.

Fig. 12 Radiation characteristics in the elevation plane (Az = 120° to 300°).

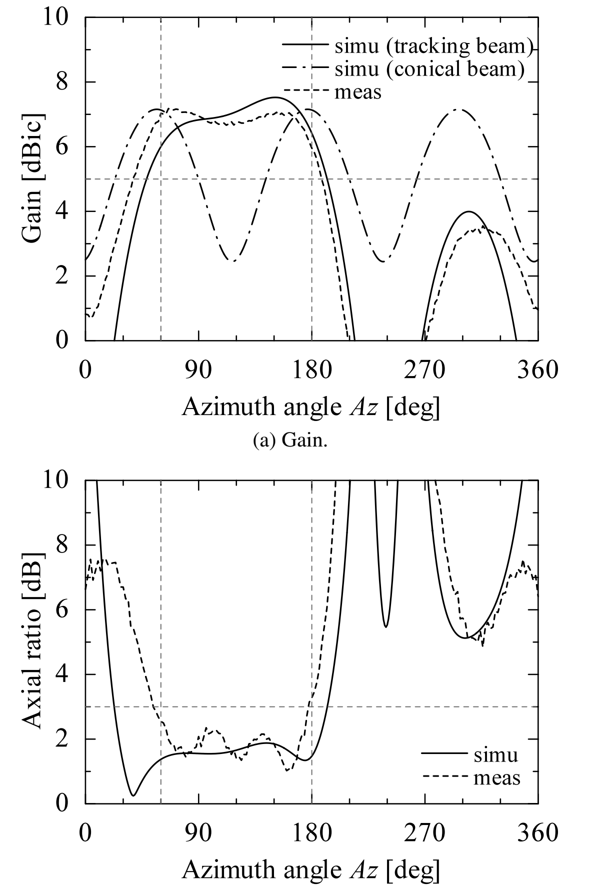

(a) Gain.

(b) Axial ratio.

Fig. 13 Radiation characteristics in the conical-cut direction (El = 48°).

4.3.5 Radiation Characteristics in the Conical-Cut Direction

Figures 13(a) and (b) represents the gain and axial ratio characteristics of the antenna for El = 48° in the case element 2 turned off. As previously, the full line and dashed line represent the results obtained by numerical simulation and measurement, respectively. In addition, the performances obtained by simulation in the case of a conical beam are plotted in dash dotted line for comparison. Figure 13(a) shows that by numerical results, the beam for which the gain is more than 5 dBic has a width of 143°. Additionally, in the same figure, it is seen that the 6 dBic gain beamwidth has a width of 124°. In the case of measurement, it is 148° and 130°, respectively. It can be seen here that when all the patches are activated, the gain of the conical beam fluctuates between 2.4 dBic and 7.2 dBic over the whole azimuth space. Moreover, from this figure, it is clear the beamwidth is insufficient to scan the whole azimuth space as requested in the specifications (Table 1) at low or medium elevation angle. Thus, it can be confirmed the use of satellite-tracking beam is more suitable to the present application as stated in the Introduction. In addition, from Fig. 13(b), the broadness of the axial ratio characteristics was confirmed by simulation and measurement as it is less than 3 dB over a range of 169° and 122° centered on 120°, respectively.

4.3.6 Verification of Beam-Switching in the Azimuth Space

The antenna characteristics were measured by turning off one of the elements from 1 to 3 in turn. By doing so, the beam-switching operation could be observed and confirmed (Fig. 14). Figure 14(a) shows the gain of the antenna in the conical-cut direction when the geostationary satellite is located at El = 48° from Tokyo. Results show that each generated beam is centered at Az = 114°, 234°, and 354° in the conical-cut direction with respect to the element that is turned off. Thus, the existence of three beams with 120° difference between them in the conical-cut direction is confirmed. In the same figure, it is seen that the minimum gain corresponding to the intersection between two adjacent beams (Az = 54°, 174°, and 294°) is 6.6 dBic. Additionally, in Fig. 14(b), the maximum axial ratio (corresponding to the maximum value obtained at each intersection of the gain as previously indicated) is 2.9 dB. Therefore, it meets

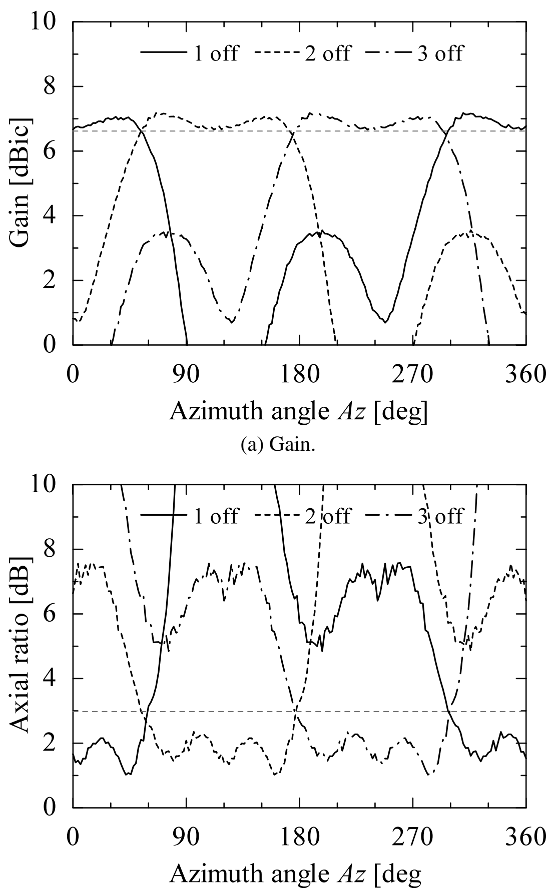

(a) Gain.

(b) Axial ratio.

Fig. 14 Beam-switching in the conical-cut direction (El = 48°).

the specification of less than 3 dB over the whole azimuth range.

Previously investigated array antennas [6]–[8], etched on a high relative permittivity substrate, cannot meet the requirements for mobile satellite communications as their surface, hence their gain, decreases too much. However, from the previously discussed results, it was confirmed that with a triangular microstrip line antenna, whose surface from the array center to the bottom edge of an element is 32% reduced compared to the previously investigated array antennas [6]–[8] (corresponding to a reduction of 20% in the case of a single element), equivalent performances could be obtained in terms of axial ratio coverage, minimum gain, etc. Note that the size reduction of the proposed triangular microstrip line antenna is due to the use of a dielectric substrate whose relative permittivity is high and due to the fact that microstrip lines are intrinsically smaller than patch antennas.

5. Conclusion

In this paper, both a single element and an array of three elements antennas, composed by a simple triangular microstrip line with a gap, able to generate a circular polarization, have been studied. A circular polarization can be simply obtained by properly adjusting the element parameters. The analysis of the array has shown that the generated beam can be switched in the azimuth space with a minimum gain of 6.6 dBic and a maximum axial ratio of 2.9 dB.

In the future, the input characteristics of the antenna will be improved by use of a microstrip line feeding or parasitic elements to tune the impedance. In addition, improvement of the antenna performances at low elevation will be researched. Furthermore, a dual-band configuration will be investigated.

Acknowledgments

This work was supported in part by the Japanese Society for the Promotion of Science, Grant-in-Aid for Scientific Research (B) number 16360185.

The authors express their special thanks to M. Amane Miura and M. Shin-ichi Yamamoto from the National Institute of Information and Communications Technology, Kashima, Japan.

References

[1] Engineering Test Satellite VIII (ETS-VIII) project, JAXA homepage (as of December 2005).
[2] K. Ito, K. Ohmaru, and Y. Konishi, "Planar antennas for satellite reception," IEEE Trans. Broad., vol.34, no.4, pp.457–464, Dec. 1988.
[3] K. Fujimoto and J.R. James, Mobile antenna systems handbook, Artech House, Boston, London, 1994.
[4] D. Delaune, T. Tanaka, T. Onishi, J.T. Sri Sumantyo, and K. Ito, "A simple satellite-tracking stacked patch array antenna for mobile communications experiments aiming at ETS-VIII applications," IEE Proc. Microw. Antennas Propag., vol.151, no.2, pp.173–179, April 2004.
[5] J.T. Sri Sumantyo, K. Ito, D. Delaune, T. Tanaka, T. Onishi, and H. Yoshimura, "Numerical analysis of ground plane size effects on patch array antenna characteristics for mobile satellite communications," Int. J. Numer. Model., vol.18, no.2, pp.95–106, March/April 2005.
[6] J.T. Sri Sumantyo and K. Ito, "Simple satellite-tracking dual-band triangular-patch array antenna for ETS-VIII applications," Radiomatics - Journal on Communications Engineering, 2005. (in press)
[7] J.T. Sri Sumantyo, K. Ito, D. Delaune, T. Tanaka, and H. Yoshimura, "Simple satellite-tracking dual-band triangular-patch array antenna for ETS-VIII applications," Proc. 2004 IEEE AP-S Int. Symp., vol.3, pp.2500–2503, Monterey, USA, June 2004.
[8] J.T. Sri Sumantyo, K. Ito, and M. Takahashi, "Dual band circularly polarized equilateral triangular patch array antenna for mobile satellite communications," IEEE Trans. Antennas. Propag., vol.53, no.11, pp.3477–3485, Nov. 2005.
[9] W. Stutzman and G. Thiele, "Antenna theory and design," chap. 5, John Wiley & Sons, New York, 1981.
[10] H. Morishita, K. Hirasawa, and T. Nagao, "A circularly polarized broadband rhombic loop antenna," IEICE Trans. Commun., vol.E79-B, no.6, pp.865–870, June 1996.
[11] H. Morishita, K. Hirasawa, and T. Nagao, "Circularly polarized wire antenna with a dual rhombic loop," IEE Proc. Microw. Antennas Propag., vol.145, no.3, pp.219–224, June 1998.
[12] R. Li, V. Fusco, and H. Nakano, "Circularly polarized open-loop antenna," IEEE Trans. Antennas. Propag., vol.51, no.9, pp.2475–2477, Sept. 2003.
[13] R. Li and V. Fusco, "Circularly polarized twisted loop antenna,"

IEEE Trans. Antennas. Propag., vol.50, no.10, pp.1377–1381, Oct. 2002.

[14] M. Sumi, K. Hirasawa, and S. Shi, "Two rectangular loops fed in series for broadband circular polarization and impedance matching," IEEE Trans. Antennas. Propag., vol.52, no.2, pp.551–554, Feb. 2004.

[15] S. Okubo and S. Tokumaru, "Reactively loaded loop antennas with reflectors for circular polarization," IEICE Trans. Commun. (Japanese Edition), vol.J65-B, no.8, pp.1044–1051, Aug. 1982.

[16] T. Tsukiji and S. Tou, "On polygonal loop antennas," IEEE Trans. Antennas. Propag., vol.AP-28, no.4, pp.571–575, July 1980.

[17] S. Tou and T. Tsukiji, "Delta loop antenna," IEICE Trans. Commun. (Japanese Edition), vol.J61-B, no.7, pp.578–584, July 1978.

[18] Y. Kumon and T. Tsukiji, "An analysis of the crossed twin delta loop antennas with circular polarization," IEICE Trans. Commun. (Japanese Edition), vol.J73-B-II, no.4, pp.190–196, April 1990.

[19] R. Li and V. Fusco, "Printed figure-of-eight wire antenna for circular polarization," IEEE Trans. Antennas. Propag., vol.50, no.10, pp.1487–1490, Oct. 2002.

[20] K. Hirose, S. Okazaki, and H. Nakano, "Double loop antenna for a circularly polarized tilted beam," IEICE Trans. Commun. (Japanese Edition), vol.J85-B, no.11, pp.1934–1943, Nov. 2002.

[21] A. Roederer, "The cross antenna: A new low-profile circularly polarized radiator," IEEE Trans. Antennas. Propag., vol.38, no.5, pp.704–710, May 1990.

[22] Y. Murakami, T. Nakamura, A. Yoshida, and K. Ieda, "Rectangular loop antenna for circular polarization," IEICE Trans. Commun. (Japanese Edition), vol.J78-B-II, no.7, pp.520–527, July 1995.

[23] H. Nakano, K. Nogami, S. Arai, H. Mimaki, and J. Yamauchi, "A spiral antenna backed by conducting plane reflector," IEEE Trans. Antennas. Propag., vol.AP-34, no.6, pp.791–796, June 1986.

[24] T. Teshirogi, M. Tanaka, and W. Chujo, "Wideband circularly polarized array with sequential rotations and phase shift of elements," Proc. Int. Symp. Antennas Propag., ISAP'85, pp.117–120, Kyoto, Japan, Aug. 1985.

[25] D. Ishide, T. Tanaka, H. Yoshimura, M. Takahashi, and K. Ito, "Beam switching characteristics of an electrical switch used in a 4 elements patch array antenna for ETS-VIII mobile station," Inst. Imag. Info. and Telev. Eng. Tech. Rep., vol.28, no.33, pp.5–8, June 2004.

[26] K. Kaneko, T. Tanaka, M. Takahashi, and K. Ito, "Beam-switching characteristics of an electrical switch used in a simple satellite-tracking triangular patch array antenna," IEICE Technical Report, vol.AP2005-79, Sept. 2005.

David Delaune was born in Le Havre, Seine Maritime, France, on June 23, 1975. He received the B.E. degree in Physics and Applications and the M.E. degree in Electronics from Universite Pierre et Marie Curie - Paris 6, Paris, France in 1998 and 1999, respectively. He is presently with the Graduate School of Science and Technology, Chiba University, Japan where he is working toward the Ph.D. degree. His main interest is the analysis and design of antennas for mobile satellite communications, small antennas and planar array antennas. He is a student member of the IEEE.

Josaphat Tetuko Sri Sumantyo was born in Bandung, Indonesia on June 25, 1970. He received the B.E. and M.E. degrees in electrical and computer engineering (ground penetrating radar systems) from Kanazawa University, Japan in 1995 and 1997, respectively, and the Ph.D. degree in artificial system sciences (applied radio wave and radar systems) from Chiba University, Japan in 2002. From 1990 to 1999, he was a Researcher with the Indonesian Governmental Agency for Assessment and Application of Technology (BPPT), in Jakarta and the Indonesian National Army (TNI-AD) in Bandung, Indonesia. He worked with the Center for Environmental Remote Sensing, Chiba University, Japan as a Research Assistant in 2000, and the Center for Frontier Electronics and Photonics, Chiba University, Japan from 2002 to 2005 as Lecturer (Post Doctoral Fellowship Researcher). He has been a Director with the Remote Sensing Research Center, Pandhito Panji Foundation (www.pandhitopanji-f.org) in Bandung, Indonesia since 2000. He is currently an Associate Professor with the Microwave Remote Sensing Laboratory, Center for Environmental Remote Sensing, Chiba University, Japan. His main interests include analysis and design of printed antennas for mobile satellite communications and ultrawide-band synthetic aperture radar (UWB-SAR), scattering wave analysis and its applications in radar remote sensing. His laboratory is also developing geographical information system for Asian Geospatial Information Database (AGID). Dr. Sri Sumantyo is a Member of the IEEE, the Japan Society for Photogrammetry and Remote Sensing (JSPRS), and the Remote Sensing Society Japan (RSSJ). He is the recipient of many awards and research grants related to his study and research.

Masaharu Takahashi was born in Chiba, Japan, on December 15, 1965. He received the B.E. degree in electrical engineering in 1989 from Tohoku University, Miyagi, Japan, and the M.E. and D.E. degrees in electrical engineering from the Tokyo Institute of Technology, Tokyo, Japan, in 1991 and 1994, respectively. He was a Research Associate from 1994 to 1996, an Assistant Professor from 1996 to 2000 with the Musashi Institute of Technology, Tokyo, Japan; and an Associate Professor from 2000 to 2004 with the Tokyo University of Agriculture and Technology, Tokyo, Japan. He is currently an Associate Professor with Chiba University, Chiba, Japan. His main interests include electrically small antennas, planar array antennas (RLSA), electromagnetic compatibility (EMC) and the research on the evaluation of the interaction between electromagnetic fields and the human body by use of numerical and experimental phantoms. Dr. Takahashi was the recipient of the 1994 IEEE Antennas and Propagation Society Tokyo Chapter Young Engineer Award. He is a senior member of the IEEE.

Koichi Ito was born in Nagoya, Japan, in June 1950. He received the B.S. and M.S. degrees from Chiba University, Chiba, Japan, in 1974 and 1976, respectively, and the D.E. degree from Tokyo Institute of Technology, Tokyo, Japan, in 1985, all in electrical engineering. From 1976 to 1979, he was a Research Associate at Tokyo Institute of Technology. From 1979 to 1989, he was a Research Associate at Chiba University. From 1989 to 1997, he was an Associate Professor at the Department of Electrical and Electronics Engineering, Chiba University, and is currently a Professor at the Research Center for Frontier Medical Engineering as well as at the Faculty of Engineering, Chiba University. In 1989, 1994, and 1998, he stayed at the University of Rennes I, France, as an Invited Professor. His main interests include analysis and design of printed antennas and small antennas for mobile communications, research on evaluation of the interaction between electromagnetic fields and the human body by use of numerical and experimental phantoms, and microwave antennas for medical applications such as cancer treatment. Dr. Ito is a Member of the AAAS, the Institute of Image Information and Television Engineers of Japan (ITE), the Japanese Society of Hyperthermic Oncology, and an IEEE Fellow. He served as Chair of Technical Group on Radio and Optical Transmissions of ITE from 1997 to 2001. He also served as Chair of the IEEE AP-S Japan Chapter from 2001 to 2002. He is now Chair of the Technical Group on Human Phantoms for Electromagnetics, IEICE, Vice-Chair of the 2007 International Symposium on Antennas and Propagation (ISAP2007), and an Associate Editor of the IEEE Transactions on Antennas and Propagation.